Journal of Petroleum Science and Engineering 169 (2018) 146–156

Contents lists available at ScienceDirect

Journal of Petroleum Science and Engineering

journal homepage: www.elsevier.com/locate/petrol

Mechanistic simulation study of expanding-solvent steam-assisted gravity drainage under reservoir heterogeneity

Arun Venkat Venkatramani, Ryosuke Okuno*

The University of Texas at Austin, USA

ARTICLE INFO

Keywords:
Steam-assisted gravity drainage
Bitumen recovery
Steam-oil ratio
Heterogeneity
Numerical simulation

ABSTRACT

Expanding-solvent steam-assisted gravity drainage (ES-SAGD) is a potential method to reduce steam-oil ratio (SOR) of SAGD, which is a critical concern especially for highly-heterogeneous reservoirs. The main objective of this research is to investigate the flow characteristics of heterogeneous reservoirs in which solvent is more likely to lower SOR of SAGD.

SAGD and ES-SAGD with normal hexane are simulated for fifty geostatistical realizations consisting of clean sand and shale, qualitatively representative of the middle member of the McMurray formation. Thermodynamic models are calibrated with experimental phase behavior data for reliable comparison between SAGD and ES-SAGD, including the water solubility in oil at elevated temperatures.

Results show that the SOR reduction by steam-solvent coinjection is positively correlated with the increase in SAGD's SOR due to heterogeneity. Enhancement of bitumen flow by dilution is more important for lowering SOR for those reservoirs in which the permeability variation makes slow-flow regions during SAGD.

Simulation results show that a larger amount of bitumen tends to be diluted by solvent in those reservoirs for which SAGD exhibits slow production of bitumen. Then, the observed results are analyzed by use of SAGD analytical equations that clarify several influential factors for bitumen flow beyond the edge of a steam chamber. It is shown that dilution of bitumen by solvent in steam-solvent coinjection becomes more significant where flow barriers limit the local bitumen flow under SAGD even at high temperatures. In such slow-flow regions, the bitumen flow rate can be substantially increased by accumulation of solvent in ES-SAGD, which reduces the oleic-phase viscosity and increases the oleic-phase saturation and, therefore, relative permeability. Solvent accumulation within a steam chamber can also reduce thermal losses because of lower operating-chamber temperatures.

1. Introduction

Steam-assisted gravity drainage (SAGD) is currently the most widely-used technique for in-situ bitumen recovery, and uses the sensitivity of bitumen viscosity to temperature (Keshavarz et al., 2014, 2015). In SAGD, a steam chamber is formed as the injected steam propagates within the reservoir. The chamber edge represents the boundary of a steam chamber, where the vapor phase condenses. Bitumen situated beyond the chamber edge is mobilized by the heat released by steam upon condensation.

The cumulative steam-oil ratio defined as the ratio of cumulative steam injected [expressed as a cold-water equivalent (CWE)] to cumulative bitumen produced is a commonly-used metric to evaluate the performance of SAGD. SOR directly correlates with thermal losses to the over- and underburden (Das, 1998; Ito and Ichikawa, 1999; Edmunds and Chhina, 2001; Butler and Yee, 2002; Gupta and Gittins, 2005; Edmunds and Peterson, 2007; Miura and Wang, 2012), and inversely correlates with the bitumen drainage rate.

In efficient SAGD projects, where the targeted formations are relatively homogeneous, the cumulative SOR is typically between 2.0 and 5.0 (Butler, 2001). SOR for SAGD is expected to be greater in highly heterogeneous reservoirs because reservoir heterogeneities result in more tortuous fluid flow. An important example of a highly heterogeneous bitumen reservoir is the middle McMurray member, which holds about 70% of the bitumen reserves within the McMurray formation (Musial et al., 2012). Prior studies on SAGD in the presence of

Abbreviations: BHP, bottom-hole pressure; BIP, binary interaction parameter; CWE, cold water equivalent; ES, expanding solvent; SAGD, steam assisted gravity drainage; hom, homogeneous case; het, heterogeneous case; SIS, sequential indicator simulation; SOR, steam-oil-ratio

* Corresponding author. Department of Petroleum and Geosystems engineering, University of Texas at Austin, CPE 5.118B, 200 E. Dean Keeton St., Stop C0300, Austin, TX, 78712-1585, USA.

E-mail address: okuno@utexas.edu (R. Okuno).

https://doi.org/10.1016/j.petrol.2018.04.074
Received 25 November 2017; Received in revised form 2 April 2018; Accepted 29 April 2018
Available online 17 May 2018
0920-4105/

permeability barriers indicate that the extent to which the SOR increases due to heterogeneity is sensitive to the size of the barriers (i.e., thickness and lateral extents) and their proximity to the SAGD well-pair (Yang and Butler, 1992; Chen et al., 2008; Yazdi and Jensen, 2014; Wang and Leung, 2015).

Lowering the SOR to meet a given cumulative bitumen production is a priority from economic and environmental standpoints. The need for lower SORs and the challenges associated with their obtainment using steam-only injection has led to the search for alternatives to SAGD. Expanding solvent-SAGD (ES-SAGD) is a widely-investigated alternative, where a small quantity of a condensable solvent is coinjected with steam. Growing interest in ES-SAGD can be attributed to two factors. Firstly, it retains many of the advantages of SAGD. Secondly, it could potentially enhance the bitumen drainage rate by the dilution of bitumen by solvent, while lowering thermal losses to the overburden through the reduction of operating-chamber temperatures (Dong, 2012; Jha et al., 2013; Keshavarz et al., 2014, 2015; Khaledi et al., 2015; Venkatramani and Okuno, 2017a; b). The combination of these two facets could lower the SOR accompanying a given cumulative bitumen production.

Mobilization of bitumen in ES-SAGD is a result of the interplay between the phase behavior of water/solvent/bitumen mixtures and fluid flow. The dilution of bitumen by solvent is driven by concentration gradients, and expedited by mechanical dispersion under high temperatures near the edge of a steam chamber. Heating of the reservoir beyond the chamber edge occurs by the mechanisms of conduction and convection; the temperature gradient available for heat transfer depends substantially on temperature along the chamber edge. The chamber edge, where the vapor phase condenses, represents the transition from oleic-vapor-aqueous (inside the chamber) to oleic-aqueous coexistence (outside the chamber). Phase equilibrium measurements and thermodynamic calculations indicate that the vapor-condensation temperature is lower than the steam-condensation temperature for a mixture of solvent, water, and bitumen at a given pressure; e.g., see Amani et al. (2013a), Brunner (1990), and Brunner et al. (2006) for fundamental data for water/oil mixtures, and Sheng et al. (2017) for such thermodynamic calculations for different solvents. These inferences have been presented by prior studies on ES-SAGD for single-component n-alkane solvents in homogeneous reservoir models (Jha et al., 2013; Keshavarz et al., 2014, 2015; Khaledi et al., 2015).

A vast majority of prior studies on ES-SAGD have been restricted to homogeneous reservoir models. Consequently, they do not address the important question of the effect of reservoir heterogeneity on the relative performance of ES-SAGD to SAGD. To our knowledge, the investigations by Li et al. (2011) and Venkatramani and Okuno (2017b) are the only detailed, systematic studies on the relative performance of ES-SAGD to SAGD under heterogeneity published in the literature.

With the aid of numerical simulations conducted for one hundred geostatistical realizations for SAGD and n-C_6 SAGD, Venkatramani and Okuno (2017b) demonstrated that (i) the SOR for ES-SAGD is less sensitive to heterogeneity compared to that for SAGD; and (ii) the reduction in SOR by steam-solvent coinjection is enhanced under heterogeneity. These simulation results were attributed to the enhanced mixing between solvent and bitumen under heterogeneity, and the interplay between solvent-bitumen mixing and temperature distribution within the reservoir.

While both Li et al. (2011) and Venkatramani and Okuno (2017b) presented useful insights on the relative performance of ES-SAGD to SAGD under heterogeneity, neither study elucidated how heterogeneous reservoirs may be identified in terms of their suitability for the application of ES-SAGD. This is an important engineering question in view of the greater cost of solvent relative to the price of bitumen. The main objective of this research is to numerically investigate the flow characteristics of heterogeneous reservoirs for which solvent coinjection is more likely to lower SOR of SAGD, and the basis underlying the effectiveness of solvent in such cases.

Section 2 presents the basic conditions for reservoir simulations conducted for fifty geostatistical realizations of a heterogeneous reservoir. Section 3 presents the main results for SAGD and n-C_6 SAGD simulations and an analysis of them with the aid of analytical equations for oleic-phase flow along the edge of a steam chamber. Section 4 summarizes the main conclusions of this research. n-C_6 is used as the solvent for ES-SAGD in this research because it has been reported to be an effective solvent for Athabasca bitumen reservoirs.

2. Simulation model

2.1. Reservoir model

Two-dimensional numerical flow simulations using STARS of Computer Modelling Group (CMG, 2011–16) are performed for a homogeneous reservoir comprising entirely of clean sand, and also for fifty geostatistical realizations of a heterogeneous reservoir consisting of clean sand (net facies) and mudstone (i.e., shale or non-net facies).

Heterogeneous realizations are generated by use of unconditional sequential indicator simulation (SIS) (Remy, 2005). The permeability barriers in this study are inclined relative to the top and basal planes of model in order to render it qualitatively representative of the middle McMurray member (Musial et al., 2012, 2013; Thomas et al., 1987). Table 1 summarizes the values assigned to the parameters pertaining to geostatistical simulations. The porosity, horizontal/vertical permeabilities, and bitumen saturation of the clean sand facies have been set to 36%, 6100 mD/3500 mD, and 85%, respectively. The corresponding values for mudstone facies are 5%, 1 mD/0.1 mD, and 15%. The consistency has been confirmed between the input values used for geostatistical simulation and properties of the simulated geological models.

The initial reservoir temperature and pressure are assumed to be 286.15 K and 15 bars, respectively. Bitumen considered in this research is “live”, comprising of a mixture of 10.22 mol% methane (C_1) and 89.78 mol% dead Athabasca bitumen. The corresponding gas-to-oil-ratio (GOR) is 5.0 m^3/m^3.

The reservoir model used is of dimensions 141 m × 500 m × 20 m in the x, y, and z directions, respectively; the y-direction represents the length along the well-pair. The model is discretized into 141 × 1 × 40 grid blocks in the x, y, and z directions, respectively. That is, each grid block is 1 m × 0.5 m in the x-z plane. This is smaller than the grid blocks of dimensions 1 m × 1 m in the x-z plane used for 2-D SAGD simulations for heterogeneous reservoirs by Deutsch (2010) and Wang and Leung (2015). The lateral, top and bottom boundaries of the reservoir model are impermeable to fluid flow.

Both the injection and production wells are situated in the 71st grid column from the left boundary of the reservoir model. The injection and production wells are respectively located in the 28th and 36th grid layers from the top of the model.

The temperature of the injected stream is equivalent to the saturation temperature of water at the operating pressure of 35 bars. The

Table 1
Input parameters for sequential indicator simulation for simple heterogeneous reservoir models comprising of clean sand and shale. The spherical model is used for the indicator variogram for the shale facies. A more detailed discussion underlying the choice of values for the parameters used for the geostatistical simulations can be found in Venkatramani and Okuno (2017b).

Property	Value
Global proportion of clean sand	0.75
Global proportion of shale	0.25
Nugget effect for indicator variogram model	0
Azimuth for variogram model	78°
Horizontal range parameter, m	12.0
Vertical range parameter, m	1.0

Table 2
Summary of the reservoir model used in simulation case studies.

Property	Value
Initial reservoir pressure at the depth of 280 m	15 bars
Initial reservoir temperature	286.15 K
Formation compressibility	1.8E-05 1/kPa
Rock heat capacity (Keshavarz et al., 2014)	2600 kJ/m^3 °C
Rock thermal conductivity (Keshavarz et al., 2014)	660 kJ/m day °C
Over/underburden heat capacity (Keshavarz et al., 2014)	2600 kJ/m^3 °C
Over/underburden thermal conductivity (Keshavarz et al., 2014)	660 kJ/m day °C
Bitumen thermal conductivity	11.5 kJ/m day °C
Gas thermal conductivity	2.89 kJ/m day °C
Producer bottom-hole pressure (minimum)	15 bars
Steam quality	0.9
Three-phase relative permeability model (CMG)	Baker's Linear Interpolation
Residual oleic-phase saturation	0.13
Critical liquid saturation for vapor-liquid relative permeability curve	0.38
Oleic-phase end-point relative permeability	1.00
Aqueous-phase end-point relative permeability	0.30
Vapor-phase end-point relative permeability	1.00
Liquid-phase end-point relative permeability	0.30

quality of steam used is 90%. The injection well is subject to the maximum bottom-hole pressure (BHP) constraint of 35 bars.

The production well is subject to a minimum BHP constraint of 15 bars, which is the initial reservoir pressure, a maximum liquid flow rate constraint of 1400 m^3/day at surface conditions, and a minimum subcool of 10 °C. For both the homogeneous and heterogeneous models, the reservoir is subject to an initial heating period of approximately 6 months using steam at 35 bars for each process, following which production is commenced. For ES-SAGD, the value of 2 mol% is used for the injection concentration of solvent.

The thermal conductivities of the overburden and underburden are set to 660 kJ/m-day-°C. Capillary pressures and asphaltene precipitation are not considered in the simulations. Phase relative permeabilities in this paper are based on Keshavarz et al. (2014). Baker's linear interpolation model (CMG, 2011–16) is used to specify the relative permeability of the oleic phase in the three-phase region. For the definition of the oleic-aqueous relative permeability curves, the irreducible aqueous-phase saturation is assumed to be equal to the initial aqueous-phase saturation of the clean sand facies. A summary of the reservoir model is presented in Table 2.

The levels of numerical dispersivities were analyzed by following the research of Garmeh (2010), Garmeh and Johns (2010), and Adepoju et al. (2015) along with dynamic simulation conditions (e.g., flow velocities and time-step sizes) for the homogeneous case and one heterogeneous realization. It was confirmed that the numerical dispersion is approximately 50% of the largest grid-block dimension, which is 0.5 m in the current reservoir model. Details of this analysis can be found in Venkatramani (2017).

Flow velocities in the vicinity of a chamber edge in the current simulation cases are on the order of several to ten cm per day. At these velocities, numerical dispersion controls components' mixing; that is, small Fickian diffusion coefficients for solvent in bitumen [e.g., 4.32×10^{-5} m^2/day for n-C_6 in bitumen (Ji et al., 2015)] has no practical significance in the current simulations.

Experimental measurements of hydrodynamic dispersion coefficients for mixtures of solvent and bitumen under gravity drainage have not been published, to the best of our knowledge. Hydrodynamic dispersivity depends at least on average particle size, local heterogeneity, and flow distance (Lake and Hirasaki, 1981; Gelhar et al., 1992; Adepoju et al., 2013). Longitudinal dispersivities were reported to range from 10^{-4} m at lab scale to 100 m at field scale (Gelhar et al., 1992; Adepoju et al., 2015). Data for transverse dispersivities are much scarcer. However, common ratios of longitudinal to transverse dispersivities are 3–30 in the literature (Gelhar et al., 1992; Grane and Gardner, 1961). A ratio of 3 was also measured by Alkindi et al. (2011) in their dispersion experiment using ethanol and glycerol, mimicking solvent dispersion in heavy oil. Then, transverse dispersivities may be estimated to range up to a few meters for typical flow distances along the edge of a steam chamber in SAGD (e.g., 10–100 m). Thus, the numerical dispersivity estimated for the current simulation model, 0.5 m, is unlikely beyond the expected range of transverse dispersivity at SAGD's field scale. No physical dispersivity of solvent in the oleic phase was specified in the simulation cases in the absence of relevant data.

2.2. Fluid model

The fluid model used in this research is based on Venkatramani and Okuno (2017a). The molecular weight of the dead Athabasca bitumen used in this research is 530 g/mol (Kumar, 2016). The dead bitumen has been characterized as a single pseudo component ("dead bitumen" component, or C_D) using the Peng-Robinson (PR) EOS (Peng and Robinson, 1976; Robinson and Peng, 1978) by Kumar and Okuno (2015). Simulations for SAGD use three components: water, C_1 and C_D. Those for ES-SAGD use four components: water, C_1, C_D, and normal hexane (n-C_6).

Compositional behavior of water/solvent/Athabasca-bitumen mixtures is modeled using the PR EOS with van der Waals' mixing rules. The dissolution of water in the oleic phase (x_{wL}) is considered to ensure reliable comparison between ES-SAGD and SAGD, following Venkatramani and Okuno (2017a). The binary interaction parameter (BIP) for water with hydrocarbons are carefully calibrated using measured phase equilibrium data (Amani et al. 2013a; b) to ensure the x_{wL} is adequately represented in flow simulations [also see Venkatramani and Okuno (2015)]. Venkatramani and Okuno (2017a) also shows details of the modeling of the viscosity and density for the oleic phase that contains C_D, water, and solvent.

The phase behavior is reflected in the simulations in terms of component equilibrium constants (or K values), defined as the ratio of concentration in one phase to another, tabulated as functions of temperature and pressure. The K values used in the simulations are independent of composition; otherwise, many simulation cases exhibit non-convergence. K values of all components corresponding to oleic-vapor-aqueous equilibrium are generated by use of the PR EOS for the fixed overall composition of 90 mol% water and 10 mol% hydrocarbons. For ES-SAGD, the overall distribution of hydrocarbons is set to 2 mol% solvent and 8 mol% live bitumen. This overall composition is considered to be representative of conditions near the chamber edge. Keshavarz et al. (2014) demonstrated that the simulated cumulative bitumen production histories are little affected by the choice of overall composition to generate K values when the mixing ratio of solvent to live bitumen in the overall mixture is in the range of 0.2–0.6.

3. Results and discussion

This section presents that the SOR reduction by steam-solvent coinjection is significantly correlated with the SOR increase due to heterogeneity under SAGD on the basis of numerical simulations for fifty realizations of a heterogeneous reservoir. The results are then explained in terms of flow characteristics ahead of the edge of a steam chamber by use of analytical equations for SAGD.

3.1. Results of SAGD and n-C_6 SAGD simulations under homogeneity and heterogeneity

Fig. 1 presents the variation of the simulated increase in SAGD's SOR due to heterogeneity (*i. e.*, $SOR_{SAGD}^{het} - SOR_{SAGD}^{hom}$) with respect to the SOR reduction by steam-solvent coinjection (*i. e.*, $SOR_{SAGD} - SOR_{ES-SAGD}$) across different realizations for the cumulative bitumen production of 42290 m^3. Statistically, the SOR reduction by steam-solvent coinjection is positively correlated with the

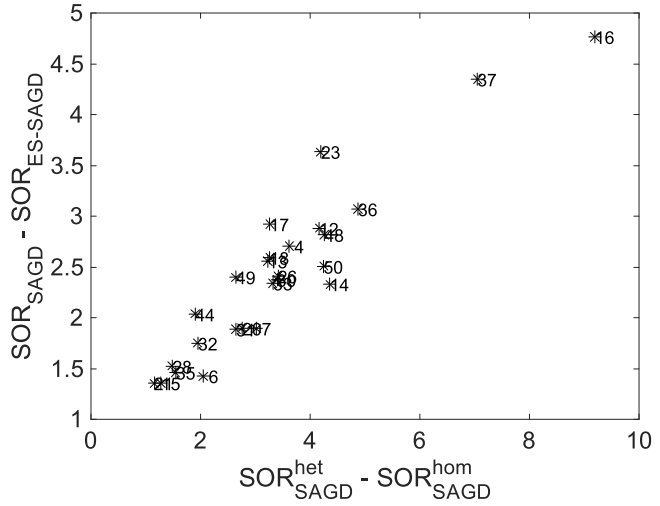

Fig. 1. SOR reduction by steam-solvent coinjection is positively correlated with the increase in SAGD's SOR due to heterogeneity.

increase in SAGD's SOR due to heterogeneity; Table S1 of Supplementary Material presents the pertinent Spearman rank correlation coefficients and p-values for several cumulative bitumen productions. Note that the number of realizations that meet a given cumulative bitumen production decreases as the cumulative bitumen production increases. This is because low-permeabilities near the well-pair in some cases result in substantially slow expansion of a steam chamber and/or because of numerical convergence issues. The latter is prevalent with simulations for ES-SAGD for heterogeneous cases. Tables S2 through S10 of Supplementary Material provide simulation results for the time taken to meet a given cumulative bitumen production and the corresponding SOR values.

The increase in SAGD's SOR due to heterogeneity is a consequence of restricted bitumen flow. Tortuous hydraulic paths for gravity drainage tend to increase the time for a unit amount of bitumen to be produced, which increases the amount of heat conduction to the over and underburden. Fig. 2 presents the variation of the increase in SAGD's SOR due to heterogeneity with the simulated bitumen production rate across different realizations for the cumulative bitumen production of 42290 m^3; Table S11 presents the pertinent statistics for several

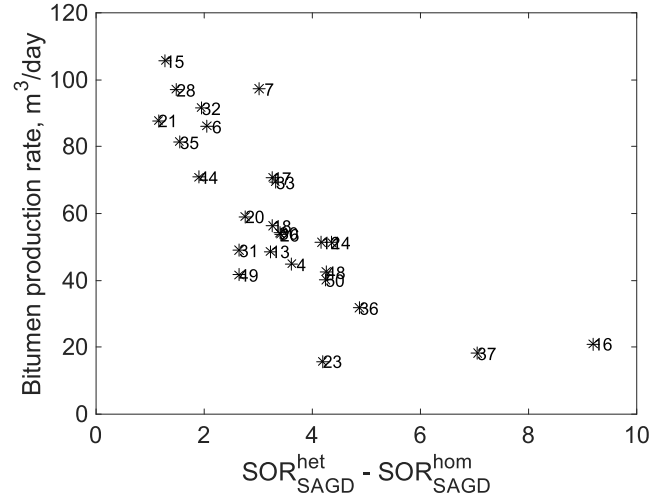

Fig. 2. Bitumen production rate in SAGD is negatively correlated with the increase in SAGD's SOR due to heterogeneity.

different cumulative bitumen productions.

For a specified cumulative bitumen production, a larger amount of solvent is retained in-situ and dissolves in the oleic phase under heterogeneity (Venkatramani and Okuno, 2017b; Venkatramani, 2017). For example, Fig. 3 compares the simulated distribution of the solvent mole fraction in the oleic phase (x_{sL}) within clean sand grid blocks for the homogeneous case and realizations 15 and 17 for the cumulative bitumen production of approximately 86124 m^3. At this cumulative bitumen production, the SOR reduction by steam-solvent coinjection is simulated to be 1.48 for the homogeneous-anisotropic case, 2.34 for realization 15, and 5.03 for realization 17. At stock-tank conditions, the volume of solvent retained in-situ is 6555 m^3 for the homogeneous-anisotropic case, 14003 m^3 for realization 15, and 22644 m^3 for realization 17. Specifically, Fig. 3a through c indicate that the areal span of high solvent concentration regions (i.e., $x_{sL} > 80$ mol% under the current operating conditions) is significantly greater under heterogeneity. Table S12 of Supplementary Material presents Spearman's rank correlation coefficients between the increase in SAGD's SOR due to heterogeneity and the number of grid blocks within the mobile zone (where oleic-phase flow rate is at least 0.05 m^3/day) with x_{sL} greater than 80 mol%. Table S12 shows that the SOR reduction by steam-solvent coinjection tends to be enhanced if a larger amount of solvent is used to dilute bitumen.

For a given steam-chamber volume (or cumulative bitumen production), the contribution of improved bitumen dilution under heterogeneity to the production rate of bitumen can be statistically demonstrated by examining the variation of the term, Δt_D, with respect to the reduction in SOR due to coinjection of solvent across different realizations. Δt_D is defined as

$$\Delta t_D(Q) = \frac{t^{het}_{SAGD}(Q) - t^{het}_{ES-SAGD}(Q)}{t^{hom}_{SAGD}(Q) - t^{hom}_{ES-SAGD}(Q)}, \quad (1)$$

where $t(Q)$ is the time taken for a given process and reservoir type (i.e., homogeneous/heterogeneous) to meet a specified cumulative bitumen production, Q. Δt_D is the normalized margin by which the time taken to meet a given cumulative bitumen production is reduced by steam-solvent coinjection for a specified reservoir. A higher value of Δt_D is indicative of increased acceleration of the production rate of bitumen relative to SAGD for the realization under consideration. The positive correlation observed in Fig. 4 indicates that the margin by which coinjection of solvent enhances the bitumen production rate also increases as the extent to which heterogeneity adversely affects the performance of SAGD increases. This figure has been created for the cumulative bitumen production of 42290 m^3. The Spearman rank correlation coefficient for this case is 0.9054 with a p-value close to zero.

The observation of simulation results from a statistical standpoint (Tables S1, S11, and S12 and Fig. 1 through 4) indicates that a larger amount of bitumen tends to be diluted by solvent in those reservoirs for which SAGD exhibits slow production of bitumen. For such cases, ES-SAGD is more likely to lower SOR of SAGD. The central hypothesis from the above observation is that there is a certain type of flow characteristics in SAGD for heterogeneous reservoirs that makes more efficient use of solvent. In what follows, the observed results will be analyzed by using a SAGD analytical model that clarifies influential factors for bitumen drainage rate along the edge of a steam chamber.

3.2. Theory

This section reviews the classical equations for bitumen drainage beyond the edge of a SAGD steam chamber at elevation z measured from the production well. Darcy's law applied to oleic-phase flow along the edge of a steam chamber is

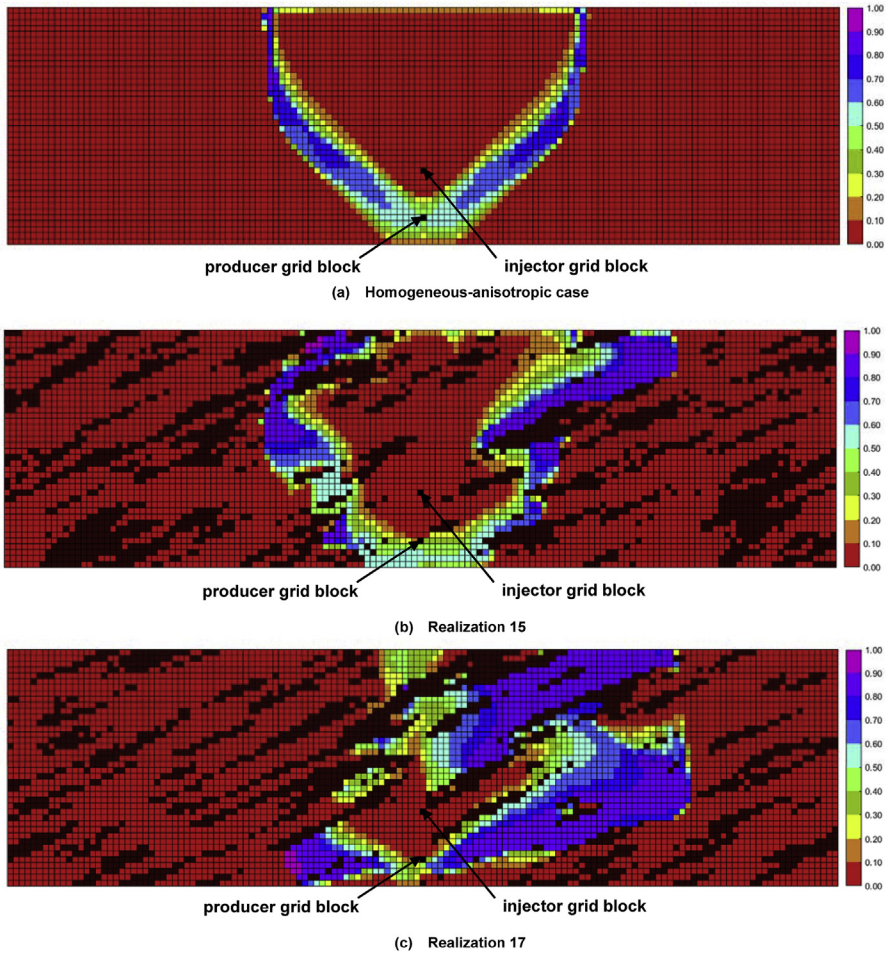

Fig. 3. Distribution of mole fraction of solvent in the oleic phase (x_{sL}) within clean sand grid blocks for different cases for the cumulative bitumen production of approximately 86124 m^3.

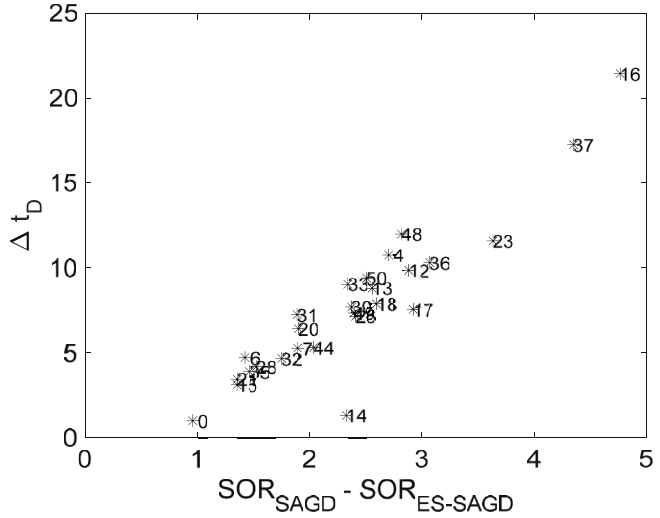

Fig. 4. Variation of Δt_D with respect to the reduction in SOR by steam-solvent coinjection across different realizations for the cumulative bitumen production of 42290 m^3.

$$U_o(z) = -k_o g \sin\theta/\nu_o, \tag{2}$$

where U_o is the oleic-phase velocity measured in the direction from the reservoir bottom to the top, k_o is oleic-phase effective permeability, g is the gravity constant, θ is the flow angle measured from the horizontal line, and ν_o is oleic-phase kinematic viscosity. Integrating U_o for a cross-section perpendicular to the edge of a steam chamber, oleic-phase flow rate at elevation z is

$$q_o(z) = \int_0^{\xi_L} U_o \Delta y d\xi = -\int_0^{\xi_L} (k_o g \sin\theta/\nu_o)\Delta y d\xi = -kg\sin\theta \Delta y I_o, \tag{3}$$

where "I_o" is defined as

$$I_o(z) = \int_0^{\xi_L} \frac{k_{ro}}{\nu_o} d\xi. \tag{4}$$

In Equations (3) and (4), Δy is the length of the horizontal section for bitumen production, ξ is the distance from the edge of a steam chamber measured in the perpendicular direction, and ξ_L is where U_o diminishes. k is permeability, and k_{ro} is oleic-phase relative permeability.

As done in previous SAGD models, 1-D steady-state heat conduction through a moving boundary (Carslaw and Jaeger, 1959) is used for transformation from ξ to temperature. That is, temperature distribution, T (ξ), along the cross-section originated at elevation z for ξ = 0 is

$$T(\xi, z) = T_R + [T_e - T_R]\exp[-\xi u/\alpha], \tag{5}$$

where T_R is the initial reservoir temperature, T_e is the local chamber-edge temperature at elevation z, u is local chamber-edge advancing velocity measured at z in the horizontal direction, and α is thermal diffusivity of the reservoir.

Use of Equation (5) with Equation (4) enables to express I_o in terms of temperature (instead of ξ), and gives the following dimensionless

variable:

$$\tau(z) = uI_o = \int_{T_L}^{T_e} \alpha k_{ro}/[\nu_o(T-T_R)]dT. \quad (6)$$

With Equation (6), Equation (3) is simplified as

$$uq_o + kg\tau\Delta y \sin\theta = 0 \quad (7)$$

for the cross-section perpendicular to the edge of a steam chamber at elevation z. Note again that u, q_o, and τ are all specified for elevation z measured from the production well. It is easy to show that the oleic-phase production rate (i.e., $-q_o$ evaluated at z = 0) is proportional to $\tau^{0.5}$ by combining Equation (7) with local and global material balance equations for a given chamber geometry (Okuno, 2015; Shi and Okuno, 2018); for example, the chamber geometries of Butler et al. (1981) and Reis (1992).

The observation in the previous section implied that steam-solvent coinjection may counter the negative impact of heterogeneity on bitumen flow in SAGD, $q_o = -kg\tau\Delta y \sin\theta/u$. Detailed analysis of individual simulation cases for different realizations have indicated that there are at least two main factors that can lower q_o under heterogeneity. Firstly, fluid flow becomes more tortuous under heterogeneity, which tends to reduce the effective reservoir hydraulic conductivity for gravity drainage in SAGD. Secondly, a larger amount of water (steam condensate) tends to accumulate in a heterogeneous reservoir. As an example, Fig. 5 shows the historical variation of the accumulated water in the reservoir for the homogeneous case and realization 17 calculated based on the injection and production histories of water at stock-tank conditions. Presence of a larger amount of water tends to lower the relative permeability to the oleic phase, k_{ro}, which reduces q_o through τ. Furthermore, if the increased accumulation of water occurs near the edge of a steam chamber, where steam condenses, the oleic-phase flow occurs at lower temperatures further away from the chamber edge. This would adversely affect q_o through the oleic-phase viscosity.

The most obvious contribution of solvent to enhancement of q_o is made through reduction of the oleic-phase kinematic viscosity, ν_o, as part of the integrand for τ. In Fig. 6, the integrand of Equation (6) with $k_{ro} = 1.0$ is plotted with respect to temperature at different dilution levels by n-C_6 for the bitumen studied. The contribution of solvent to increasing the area under the curve is calculated to be more significant at higher temperature because $1/\nu_o$ rapidly increases with increasing temperature, as is the case for bitumen. It might be somewhat counter-intuitive that the bitumen dilution can be fairly effective in enhancing

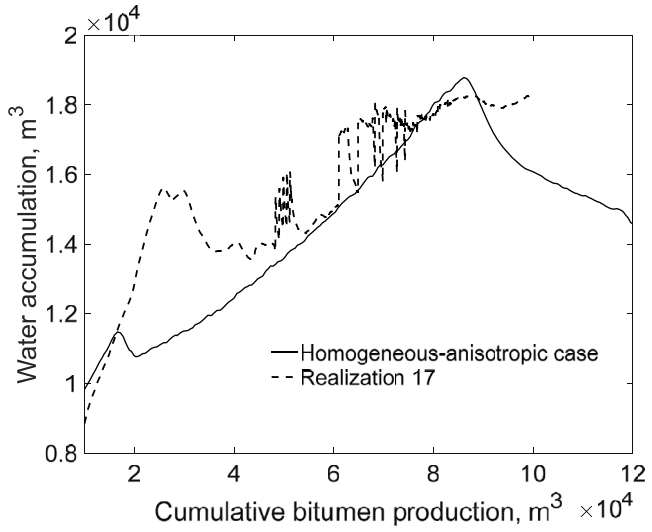

Fig. 5. Historical variation of water accumulation for the homogeneous-anisotropic case and realization 17.

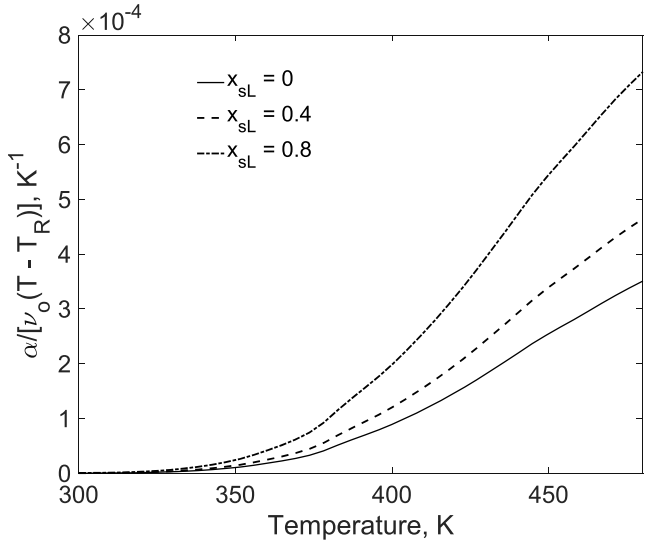

Fig. 6. The integrand of Equation (6) with $k_{ro} = 1.0$ is plotted with respect to temperature at different dilution levels by n-C_6 for the bitumen studied.

the transport of the oleic phase that is already mobile at high temperature. The next section will show that steam-solvent coinjection makes it possible to recover a certain amount of bitumen that would stay for a long time in a slow-flow region under heterogeneity in SAGD.

Another potential contribution of coinjected solvent to enhancement of q_o can be made through increasing oleic-phase saturation, which in turn increases k_{ro}. Solvent makes part of the oleic phase upon condensation, which certainly counters the adverse effect of the increased water (steam condensate) amount on q_o under heterogeneity (Fig. 5).

3.3. Discussion and analysis

The aforementioned facets are illustrated by use of the simulated property maps for realization 17 for the cumulative bitumen production of approximately 31218 m^3. This cumulative bitumen production is met at 549 days from the start of the operation for SAGD, and at 356 days for n-C_6 SAGD. The simulated cumulative SOR for SAGD for this realization and cumulative bitumen production is 6.20. When solvent is coinjected with steam for this realization, the SOR is simulated to be 3.42. That is, the SOR reduction is as much as 2.78 for this case. Figs. S1 and S2 of Supplementary Material show cumulative water injected and cumulative heat loss from the reservoir for each process for this realization and the homogeneous case.

For the SAGD process, Fig. 7 presents the simulated distribution of five different properties for realization 17 (the cumulative bitumen production is approximately 31218 m^3). Fig. 7a presents the vapor-phase saturation map predicted. In this map, clean-sand grid blocks across which a substantial change in vapor-phase saturation occurs are indicated in brown, and are designated as chamber-edge grid blocks. Fig. 7b presents the temperature distribution in clean sand grid blocks. Fig. 7c presents the distribution of molar flow rate of the bitumen component. Fig. 7de respectively give the distribution of the oleic- and aqueous-phase saturations within the clean-sand grid blocks.

Fig. 7c in conjunction with Fig. 7ab shows that the local flow of bitumen near the chamber edge in SAGD can be limited even though the oleic phase is heated to near the saturation temperature of water (515.72 K at 35 bars). That is, the thermal energy may not be enough to efficiently mobilize bitumen in slow-flow hydraulic paths. The conductivity to flow in such slow-flow paths should be enhanced by dilution to compete with higher-conductivity paths in SAGD under heterogeneity.

For realization 17, this is prominent in the highlighted region in Fig. 7a, where condensation of the vapor phase occurs near a large shale barrier. Limited bitumen flow is primarily because the shale barrier hinders the efficient transport of heated bitumen. The thickness

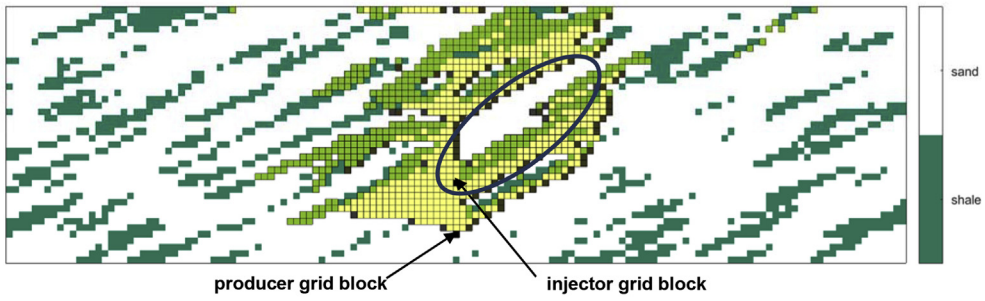

(a) Vapor-phase saturation map in SAGD for realization 17

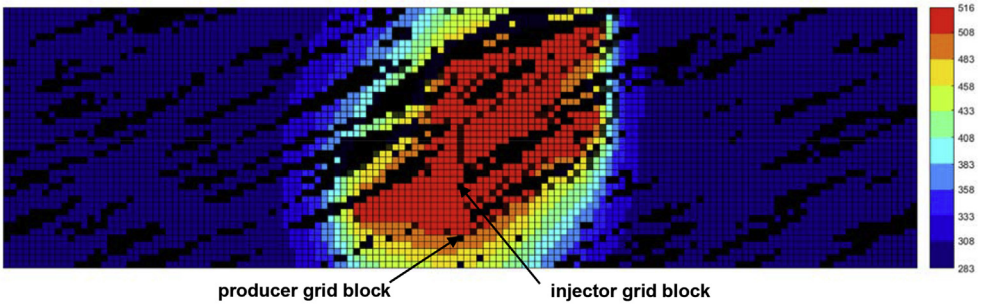

(b) Temperature distribution (in Kelvin) in clean sand grid blocks in SAGD for realization 17

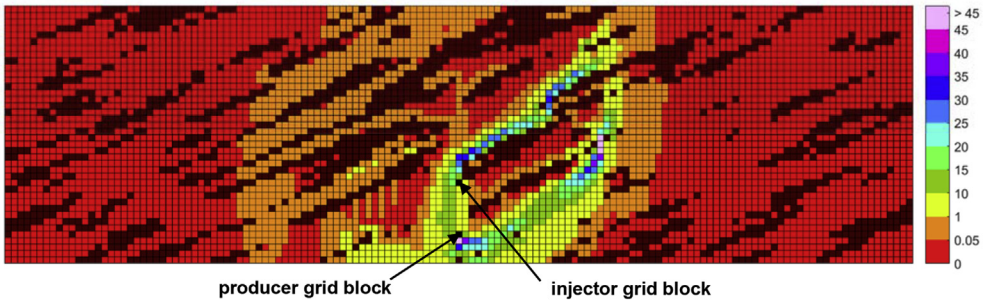

(c) Distribution of bitumen molar flow rate (kg-mole/day) in clean sand grid blocks in SAGD for realization 17

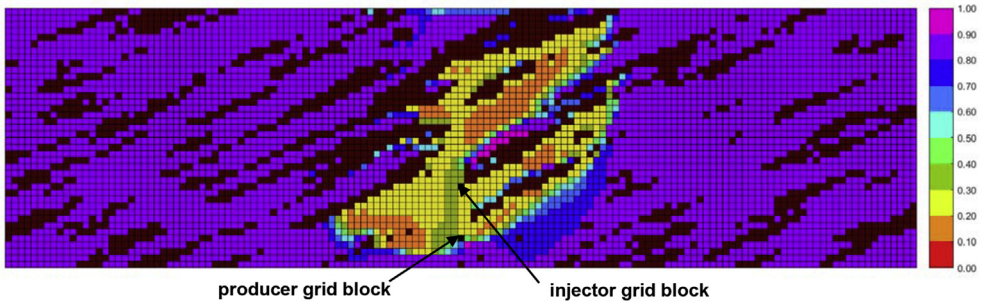

(d) Oleic-phase saturation distribution in clean sand grid blocks in SAGD for realization 17

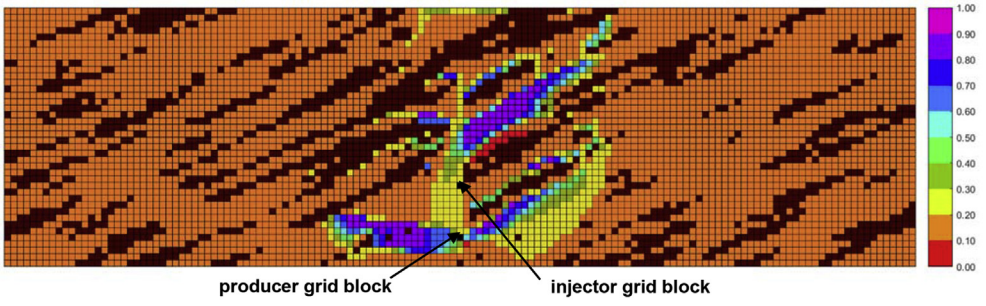

(e) Aqueous-phase saturation distribution in clean sand grid blocks in SAGD for realization 17

Fig. 7. Simulated property maps in SAGD for realization 17 for the cumulative bitumen production of approximately 31218 m^3.

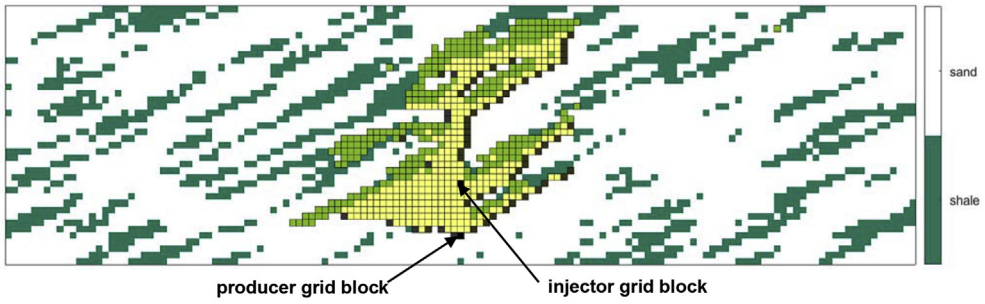

(a) Vapor-phase saturation map in n-C_6 SAGD for realization 17

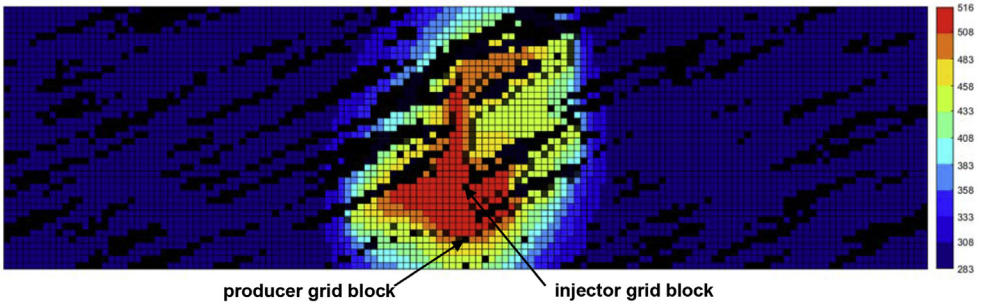

(b) Distribution of temperature (in Kelvin) in clean sand grid blocks in n-C_6 SAGD for realization 17

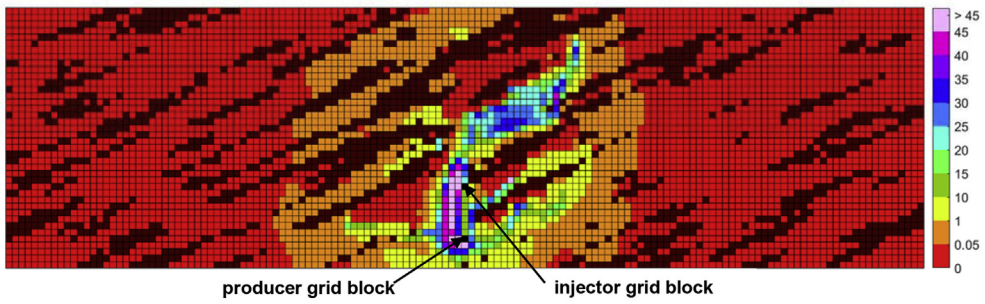

(c) Distribution of bitumen molar flow rate (kg-mole/day) in clean sand grid blocks in n-C_6 SAGD for realization 17

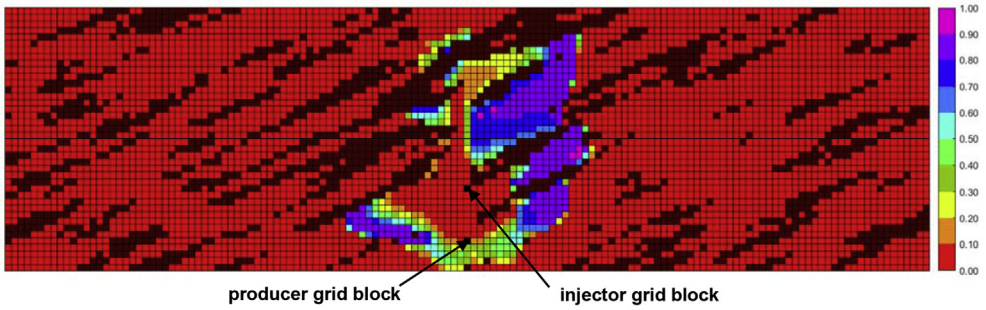

(d) Distribution of mole fraction of solvent in oleic phase (x_{sL}) in clean sand grid blocks in n-C_6 SAGD for realization 17.

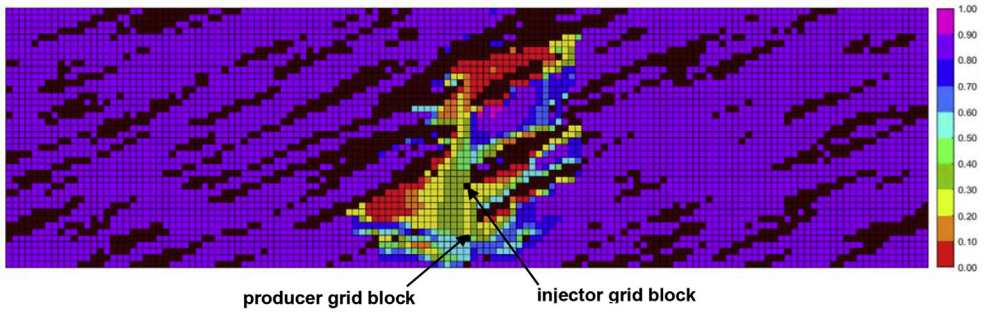

(e) Oleic-phase saturation distribution in clean sand grid blocks in n-C_6 SAGD for realization 17

Fig. 8. Simulated property maps in n-C_6 SAGD for realization 17 case for the cumulative bitumen production of approximately 31218 m^3.

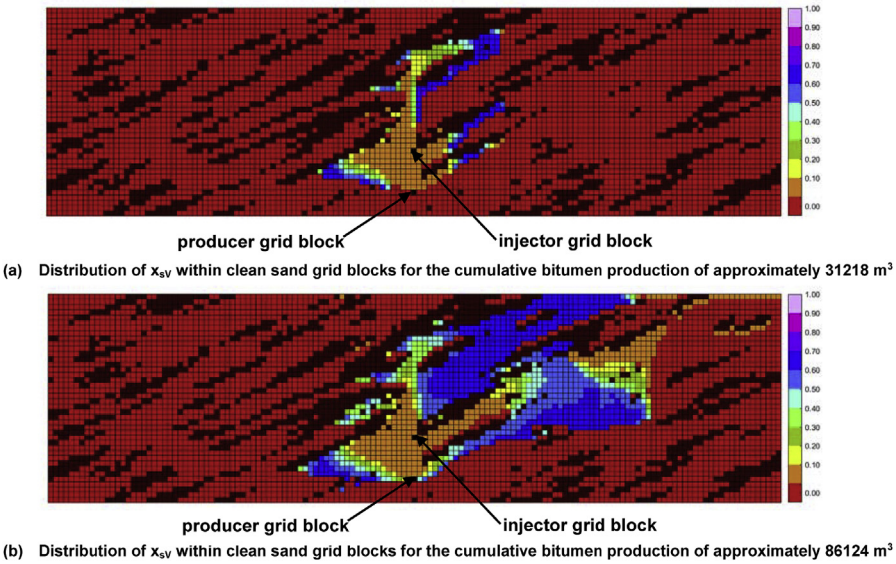

Fig. 9. Distribution of mole fraction of solvent in the vapor phase (x_{sV}) in clean sand grid blocks for realization 17 as a function of cumulative bitumen production.

of heated bitumen potentially available for flow can also be reduced due to lower oleic-phase saturations, especially when the volume of water retained in-situ is higher than that under homogeneity (Fig. 7e). For this cumulative bitumen production, the accumulation of water for the homogeneous case and realization 17 are approximately 11609 and 15108 m^3, respectively (see Fig. 5). Within the encircled region in Fig. 7a, the saturation of the aqueous phase adjacent to the chamber edge is in excess of 80%, which is detrimental to bitumen flow due to reduced oleic-phase relative permeability.

Fig. 8 presents the vapor-phase saturation, temperature, mole fraction of solvent in the oleic phase (x_{sL}), molar flow rate of bitumen, and oleic-phase saturation maps for realization 17 for n-C_6 SAGD (the cumulative bitumen production is approximately 31218 m^3). Fig. 8d indicates that the dilution of bitumen by solvent is pronounced in the heated slow-flow regions under SAGD (Fig. 7b). These maps also illustrate that the molar flow rate of bitumen is enhanced through simultaneous improvements in viscosity-reduction, and oleic-phase saturations where considerable dilution of bitumen by solvent occurs (compare Figs. 7d and 8e).

Improved reduction in the SOR due to coinjection of solvent under heterogeneity as a result of enhanced dilution is attributed to both the enhancement of the flow rate of bitumen, and reduction of thermal losses to the overburden relative to steam-only injection. Venkatramani and Okuno (2017b) demonstrated that the dilution of bitumen by solvent can lower temperatures within the reservoir by rendering the oleic phase more volatile, which facilitates the vaporization of solvent upon subsequent contact with steam. Accumulation of the solvent in the vapor phase near the chamber edge can in turn reduce the temperature at which transition from oleic-aqueous-vapor to oleic-aqueous coexistence occurs at the chamber edge.

Fig. 9 presents the distribution of the concentration of solvent in the vapor phase (x_{sV}) for the cumulative bitumen productions of approximately 31218 m^3, and 86124 m^3 for realization 17; Fig. 10 presents the pertinent distribution of temperature for SAGD and n-C_6 SAGD for the

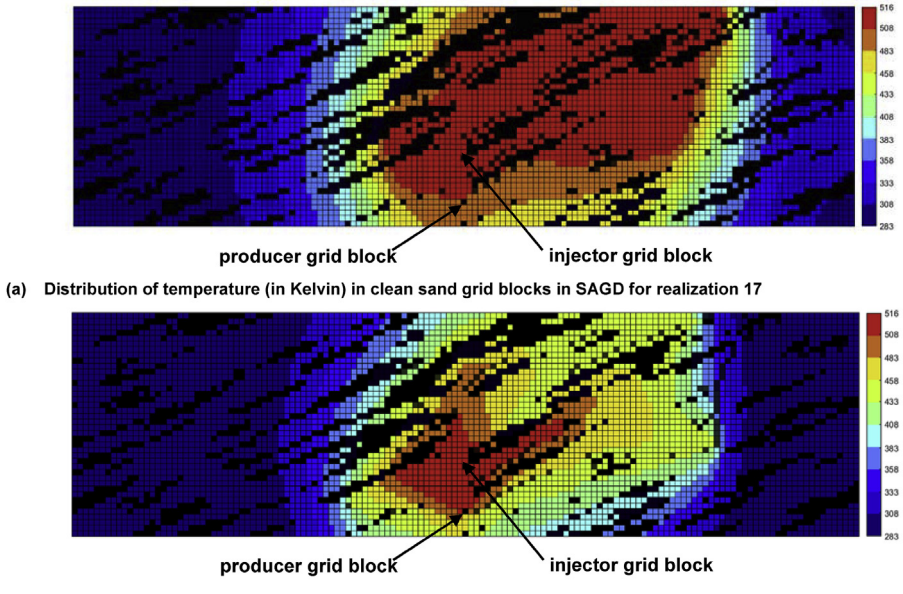

Fig. 10. Distribution of temperature in clean sand grid blocks in SAGD and n-C_6 SAGD for realization 17 for the cumulative bitumen production of approximately 86124 m^3.

cumulative bitumen production of approximately 86124 m^3. Unlike the homogeneous case, steam-rich regions wherein temperatures are comparable to the saturation temperature of water at the operating pressure need not reach the top of the formation when solvent is coinjected with steam under heterogeneity (see Fig. 7b, 8b and 10ab). Further, the margin by which the SOR is reduced due to coinjection of solvent for realization 17 is greater for the cumulative bitumen of 86124 m^3 than that for 31218 m^3 because of greater accumulation of solvent in-situ [see Figs. 3c, 8d and 9ab]. The retention of solvent for realization 17 estimated on the basis of the simulated solvent-injection and production histories at stock-tank conditions are 9893 m^3 at the cumulative bitumen production of 31218 m^3, and 22644 m^3 at 86124 m^3.

The results and discussion presented thus far indicate that the use of solvent in steam-solvent coinjection tends to be more effective in reducing the SOR under heterogeneity, but this likely requires a larger amount of solvent retention. As the cost of solvent is higher than the price of bitumen, its retrieval is important in the later stages of production. Maximization of solvent-retrieval under heterogeneity requires the development of an optimal application strategy in terms of the concentration of solvent in the injection stream (see Keshavarz et al., 2015; Venkatramani and Okuno, 2017a). Simulation studies focusing on the development of such strategies must use geological models that are conditioned by field data (e.g., well logs and seismic data) and solvents that are economically viable for field-scale implementation of ES-SAGD. Detailed development of a workflow for economically viable, field-scale implementation of ES-SAGD is beyond the scope of the current paper. Nevertheless, Venkatramani (2017) presents a potential approach to mitigate long-term solvent retention in ES-SAGD in heterogeneous reservoirs.

4. Conclusions

This paper presented a simulation study of the flow characteristics of heterogeneous bitumen reservoirs that make it more likely for steam-solvent coinjection to lower SAGD's SOR. SAGD and coinjection of steam and n-C_6 were compared mainly in terms of SOR for fifty realizations of a synthetic heterogeneous reservoir at the operating pressure of 35 bars, and 2 mol% for the injection concentration of solvent. Mechanistic explanation of the results was based on analytical equations for bitumen flow beyond the edge of a SAGD steam chamber, which clarified how steam-solvent coinjection can contribute to enhancement of bitumen flow under heterogeneity. Conclusions of this research are as follows:

- Simulation results statistically showed that SOR reduction by steam-solvent coinjection is expected to be more significant if SAGD's SOR is more significantly increased by the presence of permeability barriers. For such cases, enhancement of bitumen flow is crucial for lowering SOR, and is possible with steam-solvent coinjection.
- For the heterogeneous reservoir models and operating conditions used in this research, the margin by which the SOR is reduced as a result of coinjection of n-C_6 is at least 2.0 when the average increase in SAGD's SOR due to heterogeneity is 2.45.
- A larger amount of solvent tends to accumulate if SAGD in the reservoir results in higher SOR in the presence of permeability barriers. Such accumulation of solvent was particularly observed in slow-flow regions near permeability barriers, where steam-only injection did not make bitumen mobility sufficiently high for efficient transport of the bitumen to fast-flow regions.
- Analysis of SAGD equations for bitumen flow indicates that the enhancement of bitumen flow by dilution is more pronounced at higher temperature. This comes mainly from the rapid reduction of the bitumen kinematic viscosity with increasing temperature.
- The solvent accumulation also counters the adverse effect of the increased water accumulation in heterogeneous cases by increasing the oleic-phase saturation, therefore, relative permeability.
- Enhanced dilution of bitumen by solvent under heterogeneity reduces the SOR both through the improvement of molar flow rate of bitumen and reduction of thermal losses to the overburden.

Acknowledgements

We gratefully acknowledge the financial support from Japan Petroleum Exploration Co., Ltd. and Japan Canada Oil Sands Ltd. We are also grateful to Dr. Juliana Leung at University of Alberta for assisting us with SIS. Ryosuke Okuno holds the Pioneer Corporation Faculty Fellowship on Petroleum Engineering at The University of Texas at Austin.

Nomenclature

Roman symbols

I	term related to relative effects of heat transfer to fluid flow in Equation (3)
g	acceleration due to gravity
k	absolute permeability
q	volumetric flow rate
Q	cumulative bitumen production
U	velocity
x	mole fraction
z	vertical distance
T	temperature

Greek symbols

τ	dimensionless parameter in Equation (6)
θ	angle subtended by chamber edge
ξ	distance

Subscripts

edge	chamber edge
s	solvent
o	oil

Appendix A. Supplementary data

Supplementary data related to this article can be found at http://dx.doi.org/10.1016/j.petrol.2018.04.074.

References

Adepoju, O.O., Lake, L.W., Johns, R.T., 2013. Investigation of Anisotropic mixing in miscible displacements. SPE Reservoir Eval. Eng. 16 (01), 85–96.
Adepoju, O.O., Lake, L.W., Johns, R.T., 2015. Anisotropic dispersion and upscaling for miscible displacement. SPE J. 20 (03), 421–432.
Alkindi, A.S., Al-Wahaibi, Y.M., Muggeridge, A.H., 2011. Experimental and numerical investigations into oil drainage rates during vapor extraction of heavy oils. SPE J. 16 (02), 343–357.
Amani, M.J., Gray, M.R., Shaw, J.M., 2013a. Phase behavior of Athabasca bitumen water mixtures at high temperature and pressure. J. Supercrit. Fluids 77, 142–152.
Amani, M.J., Gray, M.R., Shaw, J.M., 2013b. Volume of mixing and solubility of water in Athabasca bitumen at high temperature and pressure. Fluid Phase Equil. 358, 203–211.
Brunner, E., 1990. Fluid mixtures at high pressures IX. Phase separation and critical phenomena in 23 (n-Alkane + water). Mixtures. The Journal of Chemical Thermodynamics 22 (4), 335–353.
Brunner, E., Thies, M.C., Schneider, G.M., 2006. Fluid mixtures at high pressures: phase behavior and critical phenomena for binary mixtures of water with aromatic hydrocarbons. J. Supercrit. Fluids 39 (2), 160–173.
Butler, R.M., 2001. Some recent developments in SAGD. J. Can. Petrol. Technol. 40 (1), 18–22.
Butler, R.M., Yee, C.T., 2002. Progress in the in situ recovery of heavy oils and bitumen. J. Can. Petrol. Technol. 41 (01), 31–40.
Butler, R.M., McNab, G.S., Lo, H.Y., 1981. Theoretical studies on the gravity drainage of heavy oil during in-situ steam heating. Can. J. Chem. Eng. 59, 455–460.
Carslaw, H.S., Jaeger, J.C., 1959. Conduction of Heat in Solids, second ed. Oxford Science Publications.
Chen, Q., Gerritsen, M.G., Kovscek, A.R., 2008. Effects of reservoir heterogeneities on the

steam-assisted gravity-drainage process. SPE Reservoir Eval. Eng. 11 (05), 921–932.
Computer Modeling Group, 2011-16. STARS Version 2011-16 User Guide. CMG, Calgary, Alberta, Canada.
Das, S.K., 1998. Vapex: an efficient process for the recovery of heavy oil and bitumen. SPE J. 3 (03), 232–237.
Deutsch, C.V., 2010. Estimation of vertical permeability in the McMurray formation. J. Can. Petrol. Technol. 49 (12), 10–18.
Dong, L., 2012. Effect of vapour–liquid phase behaviour of steam–light hydrocarbon systems on steam assisted gravity drainage process for bitumen recovery. Fuel 95, 159–168.
Edmunds, N., Chhina, H., 2001. Economic optimum operating pressure for SAGD projects in Alberta. J. Can. Petrol. Technol. 40 (12), 14–17.
Edmunds, N., Peterson, J., 2007. A unified model for prediction of CSOR in steam-based bitumen recovery. In: Presented at Canadian International Petroleum Conference. Petroleum Society of Canada PETSOC-2007-027.
Garmeh, G., 2010. Investigation of Scale Dependent Dispersivity and its Impact on Upscaling Miscible Displacements (PhD thesis). The University of Texas at Austin.
Garmeh, G., Johns, R.T., 2010. Upscaling of miscible floods in heterogeneous reservoirs considering reservoir mixing. SPE Reservoir Eval. Eng. 13 (05), 747–7643.
Gelhar, L.W., Welty, C., Rehfeldt, K.R., 1992. A critical review of data on field-scale dispersion in aquifers. Water Resour. Res. 28 (7), 1955–1974.
Grane, F.E., Gardner, G.H.F., 1961. Measurements of transverse dispersion in granular media. J. Chem. Eng. Data 6 (2), 283–287.
Gupta, S.C., Gittins, S.D., 2005. Christina lake solvent aided process pilot. In: Presented at Canadian International Petroleum Conference, PETSOC-2005-190.
Ito, Y., Ichikawa, M., Hirata, T., 1999. The effect of gas injection on oil recovery during SAGD projects. In: Presented at Annual Technical Meeting. Petroleum Society of Canada PETSOC-99–19.
Jha, R.K., Kumar, M., Benson, I., Hanzlik, E., 2013. New insights into steam/solvent-coinjection-process mechanism. SPE J. 18 (05), 867–877.
Ji, D., Dong, M., Chen, Z., 2015. Analysis of steam–solvent–bitumen phase behavior and solvent mass transfer for improving the performance of the ES-SAGD process. J. Petrol. Sci. Eng. 133, 826–837.
Keshavarz, M., Okuno, R., Babadagli, T., 2014. Efficient oil displacement near the chamber edge in ES-SAGD. J. Petrol. Sci. Eng. 118, 99–113.
Keshavarz, M., Okuno, R., Babadagli, T., 2015. Optimal application conditions for steam/solvent coinjection. SPE Reservoir Eval. Eng. 18 (01), 20–38.
Khaledi, R., Boone, T.J., Motahhari, H.R., Subramanian, G., 2015. Optimized solvent for solvent assisted-steam assisted gravity drainage (SA-SAGD) recovery process. In: Presented at SPE Heavy Oil Technical Conference, SPE 174429-MS.
Kumar, A., 2016. Characterization of Reservoir Fluids Based on Perturbation from N-Alkanes (PhD thesis). The University of Alberta.
Kumar, A., Okuno, R., 2015. Direct perturbation of the peng-Robinson attraction and covolume parameters for reservoir fluid characterization. Chem. Eng. Sci. 127, 293–309.
Lake, L.W., Hirasaki, G.J., 1981. Taylor's dispersion in stratified porous media. SPE J. 21 (04), 459–468.
Li, W., Mamora, D., Li, Y., Qiu, F., 2011. Numerical investigation of potential injection strategies to reduce shale barrier impacts on SAGD process. Journal of Canadian Petroleum Technology 50 (03), 57–64.
Miura, K., Wang, J., 2012. An analytical model to predict cumulative steam/oil ratio (CSOR) in thermal-recovery SAGD process. Journal of Canadian Petroleum Technology 51 (04), 268–275.
Musial, G., Reynaud, J.Y., Gingras, M.K., Féniès, H., Labourdette, R., Parize, O., 2012. Subsurface and outcrop characterization of large tidally influenced point bars of the cretaceous McMurray formation (Alberta, Canada). Sedimentary Geology 279, 156–172.
Musial, G., Labourdette, R., Franco, J., Reynaud, J.Y., 2013. Modelling of a tide- influenced point bar heterogeneity distribution and impacts on steam-assisted gravity drainage production: example from steepbank river, McMurray formation, Canada. AAPG Studies in Geology 64, 545–564.
Okuno, R., 2015. Class Notes for “Thermal Methods for Heavy Oil Recovery”. University of Alberta PET E 478.
Peng, D.Y., Robinson, D.B., 1976. A new two-constant equation of state. Industrial and Engineering Chemistry Fundamentals 15 (1), 59–64.
Reis, J.C., 1992. A steam-assisted gravity drainage model for tar sands: linear geometry. The Journal of Canadian Petroleum Technology 31 (10), 14–20.
Remy, N., 2005. S-GeMS: the stanford geostatistical modeling software: a tool for new algorithms development. In: Geostatistics Banff 2004 Springer Netherlands, pp. 865–871.
Robinson, D.B., Peng, D.Y., 1978. The Characterization of the Heptanes and Heavier Fractions for the GPA Peng-Robinson Programs. Gas Processors Association Research Report RR-28. .
Sheng, K., Okuno, R., Wang, M., 2017. Water-soluble solvent as an additive to steam for improved SAGD. In: SPE Canada Heavy Oil Technical Conference, SPE-184983-MS.
Shi, X., Okuno, R., 2018. Analytical solution for steam-assisted gravity drainage with consideration of temperature variation along the edge of a steam chamber. Fuel 217, 262–274.
Thomas, R.G., Smith, D.G., Wood, J.M., Visser, J., Calverley-Range, E.A., Koster, E.H., 1987. Inclined heterolithic stratification—terminology, description, interpretation and significance. Sedimentary Geology 53 (1–2), 123–179.
Venkatramani, A., 2017. Steam-solvent Coinjection for Bitumen Recovery under Reservoir Heterogeneity with Consideration of Water Solubility in Oil. The University of Alberta (PhD thesis). https://www.dropbox.com/s/5q4edjj38u2saws/Venkatramani_Arun%20Venkat_201709_PhD.pdf?dl=0 Accessed November 06 2017.
Venkatramani, A., Okuno, R., 2015. Characterization of water-containing oil using an EOS for steam injection processes. Journal of Natural Gas Science and Engineering 26, 1091–1106.
Venkatramani, A., Okuno, R., 2017a. Compositional mechanisms in steam-assisted gravity drainage and expanding-solvent steam-assisted gravity drainage with consideration of water solubility in oil. SPE Reservoir Evaluation & Engineering 20 (03), 681–697.
Venkatramani, A., Okuno, R., 2017b. In: Steam-solvent Coinjection under Heterogeneity: Should ES-SAGD Be Implemented for Highly Heterogeneous Reservoirs? Presented at SPE Heavy Oil Technical Conference, SPE 185001-MS.
Wang, C., Leung, J., 2015. Characterizing the effects of lean zones and shale distribution in steam-assisted-gravity-drainage recovery performance. SPE Reservoir Evaluation & Engineering 329–345.
Yang, G., Butler, R.M., 1992. Effects of reservoir heterogeneities on heavy oil recovery by steam-assisted gravity drainage. Journal of Canadian Petroleum Technology 31 (08), 37–43.
Yazdi, M.M., Jensen, J.L., 2014. Fast screening of geostatistical realizations for SAGD reservoir simulation. Journal of Petroleum Science and Engineering 124, 264–274.